JACS JOURNAL OF THE AMERICAN CHEMICAL SOCIETY
ARTICLE
pubs.acs.org/JACS

Reactivity of Metallic Nitride Endohedral Metallofullerene Anions: Electrochemical Synthesis of a $Lu_3N@I_h\text{-}C_{80}$ Derivative

Fang-Fang Li,[†] Antonio Rodríguez-Fortea,[‡] Josep M. Poblet,[*,‡] and Luis Echegoyen[*,†]

[†]Department of Chemistry, University of Texas at El Paso, El Paso, Texas 79968, United States
[‡]Departament de Química Física i Inorgànica, Universitat Rovira i Virgili, 43007 Tarragona, Spain

Supporting Information

ABSTRACT: Electrochemically generated $Lu_3N@I_h\text{-}C_{80}$ dianions react with the electrophile, $PhCHBr_2$, to produce a methano derivative of $Lu_3N@I_h\text{-}C_{80}(CHC_6H_5)$ (**1**) with high regioselectivity. The compound was characterized by MALDI-TOF, NMR, and UV−vis−NIR absorption spectroscopy. Electrochemical characterization of this $Lu_3N@I_h\text{-}C_{80}(CHC_6H_5)$ derivative showed the typical irreversible reductive behavior of the pristine $Lu_3N@I_h\text{-}C_{80}$, similar to those observed for Bingel adducts of $Lu_3N@I_h\text{-}C_{80}$. Using the same conditions, the reaction between $Sc_3N@I_h\text{-}C_{80}$ dianions and $PhCHBr_2$ was conducted for comparison. Unexpectedly, no nucleophilic reaction was observed, indicating that $Sc_3N@I_h\text{-}C_{80}$ dianions are not reactive toward the electrophile. Theoretical studies for both dianionic $Lu_3N@I_h\text{-}C_{80}$ and $Sc_3N@I_h\text{-}C_{80}$ showed that the HOMO is more highly localized on the fullerene cage for $[Lu_3N@I_h\text{-}C_{80}]^{2-}$ and more localized on the inside cluster for $[Sc_3N@I_h\text{-}C_{80}]^{2-}$, providing an explanation for the drastically different reactivities observed.

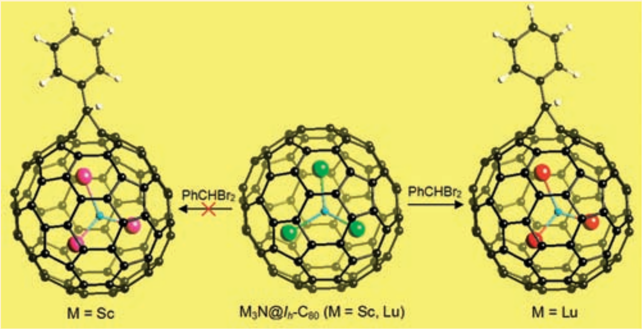

INTRODUCTION

Due to the potential applications of trimetallic nitride template endohedral metallofullerene (TNT-EMF)[1−4] derivatives in photovoltaics,[5−10] medical diagnostics and radiotheraphy,[11−15] and medicinal chemistry,[16,17] the preparation of functionalized TNT-EMFs and development of new methods for their synthesis are important. Derivatization of endohedral metallofullerenes has only been focused on cycloaddition reactions, for example, Diels−Alder,[18,19] 1,3-dipolar,[20−28] cyclopropanation,[29−32] [2 + 2]-addition,[33] and free radical additions reactions.[29,34−37] Exploring new strategies to functionalize TNT metallofullerenes is crucial to prepare novel derivatives for potential applications.

Fullerene anions can be easily generated by either chemically or electrochemically reductive methods.[38,39] Electrochemical reduction is convenient since it is easy to generate the desired anions by controlling the potential and charge transferred, *q*, to the fullerene cages. Anionic C_{60} and C_{70} have been used as nucleophilic reagents for fullerene functionalizations. The first report of the functionalization of a fullerene using anions generated under controlled potential bulk electrolysis conditions was reported in 1993 by Kadish et al., and 1,2- and 1,4-$(CH_3)_2C_{60}$ were synthesized electrosynthetically.[40] Subsequently, the reactions of $C_{60}{}^{2-}$ and $C_{70}{}^{2-}$ with a variety of organic halides[41−47] were extensively explored. In 2008, Gao et al. found an unexpected reactivity of $C_{60}{}^{3-}$ in benzonitrile solution and a novel heterocyclic derivative of C_{60} was characterized.[48] This observation was followed up with a study using $[C_{61}HPh]^{3-}$ instead of pristine $C_{60}{}^{3-}$ as the starting material in benzonitrile, *m*-methoxybenzonitrile, *m*-tolunitrile, and *o*-tolunitrile, and four fullerooxazoles were regioselectively formed.[49,50] More recently, this research group reported that the reaction of $C_{60}{}^{2-}$ with the same organic halides in different solvents can give rise to different products.[47] These results clearly show the potential importance of fullerene anions as reagents to prepare functionalized fullerenes which are difficult to prepare in other ways. The chemistry of anionic fullerenes is an important complement to that of neutral species.

While the reactivity of anionic empty fullerenes is reasonably well developed, the corresponding endohedral metallofullerene anions remain completely unexplored. This prompted us to study the reactivity of TNT-EMF anions, paying particular attention to the effect, if any, of the nature of the encapsulated metallic nitride clusters. We describe here the first derivative of $Lu_3N@I_h\text{-}C_{80}$ obtained from the nucleophilic reaction of $[Lu_3N@I_h\text{-}C_{80}]^{2-}$ generated under controlled potential electrolysis (CPE). In addition, and in marked contrast, we found that $[Sc_3N@I_h\text{-}C_{80}]^{2-}$ under the same conditions did not react at all. Thus, the $Sc_3N@I_h\text{-}C_{80}$ dianion is much less reactive with electrophiles than the $Lu_3N@I_h\text{-}C_{80}$ dianion. Computational studies of both dianionic TNT metallofullerenes showed that the electronic structures are very different for these compounds, providing a clear explanation for the different reactivities and the strong influence of the endohedral cluster on the exohedral chemistry.

Received: November 19, 2010
Published: February 3, 2011

Scheme 1. Electrosynthesis of [Methano-[6,6]-Lu_3N@I_h-C_{80}]fullerene under Controlled Potential Electrolysis

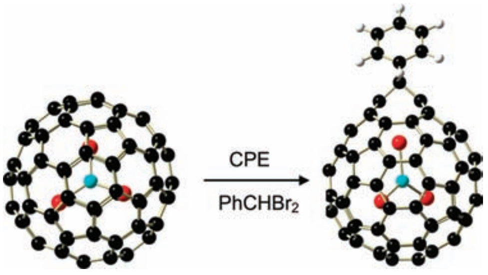

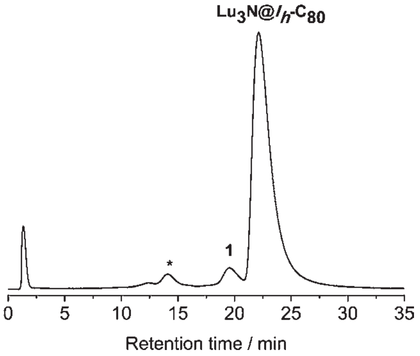

Figure 1. HPLC profile of the crude mixture obtained from the reaction between Lu_3N@I_h-C_{80} dianion and $C_6H_5CHBr_2$ using a PBB column, eluted with toluene at a flow rate of 3 mL min^{-1}. The peak labeled with an asterisk (*) is a mixture and has not been characterized.

RESULTS AND DISCUSSION

Synthesis and Isolation of [Methano-[6,6]-Lu_3N@I_h-C_{80}]-fullerene (1). It has been proposed that the C_{80} cage of TNT-EMFs is stabilized by the transfer of six electrons from the encapsulated trimetallic nitride cluster to the fullerene cage, which results in closed-shell electronic structures, i.e., $(M_3N)^{6+}C_{80}{}^{6-}$,[24,51−54] with high stabilities and low reactivities. Therefore, the procedures used for the synthesis of methanofullerene $C_{61}HPh$[46] had to be significantly modified to obtain the desired Lu_3N@I_h-C_{80} derivatives. A 4 mg sample of Lu_3N@I_h-C_{80} was reduced in *o*-dichlorobenzene (*o*-DCB) and *N,N*-dimethylfomamide (DMF) containing 0.05 M tetra-*n*-butylammonium-hexafluorophosphate, *n*-Bu_4NPF_6, as the supporting electrolyte under controlled potential electrolysis (CPE) at −1.60 V under an argon atmosphere (Scheme 1). The potentiostat was switched off after the electrogeneration of $[Lu_3N$@I_h-$C_{80}]^{2-}$ was completed, an excess of benzal bromide ($PhCHBr_2$) was then added to the solution in one portion, and the reaction was allowed to proceed for 2 h with stirring. A large amount of methanol was then added to precipitate the product. The slurry was separated by filtration, and the residue was put in toluene and sonicated. The soluble fraction was purified by HPLC using a PBB column as shown in Figure 1.

The matrix-assisted laser desorption ionization time-of-flight (MALDI-TOF) mass spectrum of **1** exhibits a protonated molecular ion peak at *m*/*z* 1589.81 corresponding to the benzal ($-CHC_6H_5$) derivatized Lu_3N@I_h-C_{80}. The peak at 1499.67 is attributed to the protonated Lu_3N@I_h-C_{80} formed by loss of the benzal group from **1**. On the basis of the mass value, **1** is a benzal group (PhHC−) monoadduct derivative of Lu_3N@I_h-C_{80}. Functionalization of the I_h isomer of C_{80} could lead to two different regioisomers depending on the addition site, either a [5,6]- or a [6,6]-ring junction, which cannot be distinguished based on the MALDI-TOF mass spectrum.

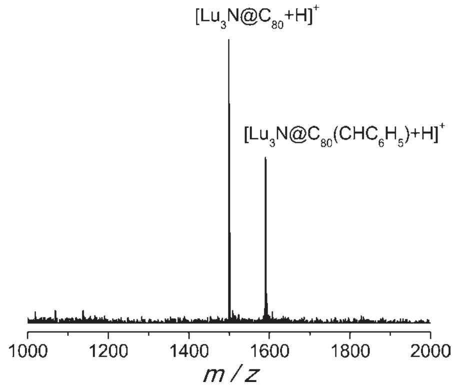

Figure 2. Positive ionization mode MALDI-TOF mass spectrum of **1**.

Scheme 2. Possible Regioisomeric Monoadducts of Lu_3N@I_h-C_{80} (from left to right: 6,6-adducts (a) and 5,6-adducts (b))

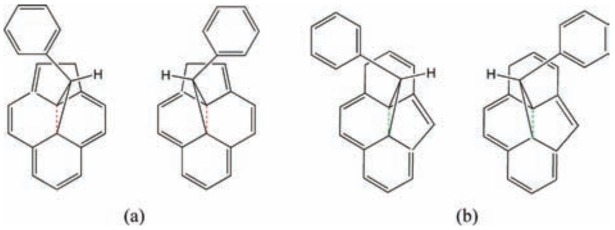

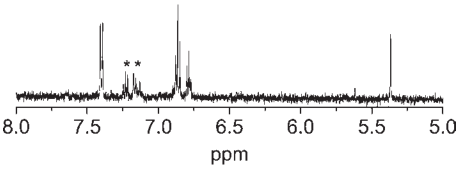

Figure 3. Proton NMR spectrum of **1**. The peaks labeled with asterisk (*) are from the toluene used during HPLC purification.

[6,6]-Addition on an I_h-C_{80} cage produces a pair of enantiomers (Scheme 2a) indistinguishable by NMR spectroscopy, whereas the [5,6]-addition leads to constitutional isomers (Scheme 2b); the hydrogen atom would be on top of either a five- or a six-membered ring. The latter would exhibit different NMR patterns due to the differences in the electronic surface currents and have very different chemical shifts. The ^1H NMR spectrum of **1** recorded in acetone-d_6/CS_2 showed a single set of signals, which suggest a [6,6]-addition pattern on the I_h-C_{80} cage. As illustrated in Figure 3, the methine proton is characterized by a singlet resonance at 5.37 ppm, which is consistent with the reported resonance at 5.38 ppm of the methine proton of $C_{61}HPh$.[46] Resonances corresponding to the phenyl protons appear at 7.40 (d, *J* = 8.5 Hz, 2H), 6.86 (t, *J* = 7.5 Hz, 1H), and 6.78 (t, *J* = 7.5 Hz, 2H) ppm with an integration ratio of 2:2:1. The ratio of the peak area of the methine proton to that of the

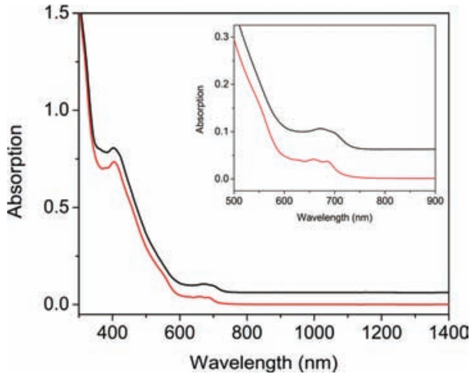

Figure 4. Absorption spectra of $Lu_3N@I_h$-C_{80} (black) and [methano-[6,6]-$Lu_3N@I_h$-C_{80}]fullerene (red).

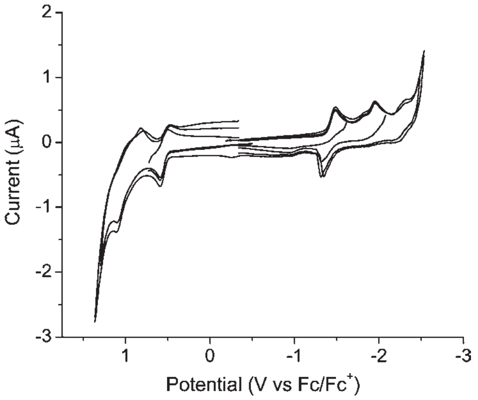

Figure 5. Cyclic voltammogram of **1**. The voltammogram was recorded in a 0.05 M solution of *n*-Bu_4NPF_6 in *o*-DCB at a scan rate of 100 mV/s.

Table 1. Redox Potentials of $Lu_3N@I_h$-C_{80} and Product 1 versus Fc/Fc$^+$

	$E^{+/2+}$ [V]	$E^{0/+}$ [V]	$E^{0/-}$ [V]	$E^{-/2-}$ [V]	$E^{2-/3-}$ [V]
$Lu_3N@I_h$-C_{80} [a]	+1.11 [b]	+0.64 [b]	−1.42 [b]	−1.80 [b]	−2.26 [b]
1	+1.10 [c]	+0.59 [c]	−1.49 [b]	−1.95 [b]	−2.32 [b]

[a] From ref 30. [b] Peak potential. [c] Quasi-reversible process.

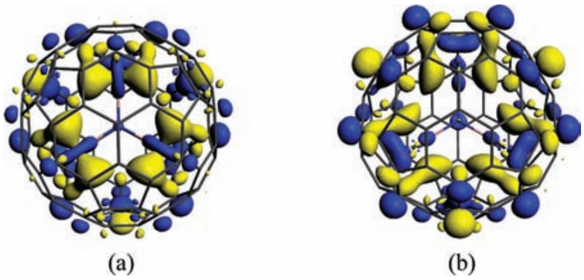

Figure 6. Representation of the HOMOs for $[Sc_3N@I_h$-$C_{80}]^{2-}$ (a) and $[Lu_3N@I_h$-$C_{80}]^{2-}$ (b).

phenyl protons is 1:5, consistent with the structure of the benzal group. On the basis of symmetry considerations, the observed NMR signals are consistent with a [6,6]-addition pattern but it is not clear whether the compound is a cyclopropane derivative or an open cage fulleroid, because the ^{13}C NMR spectrum was not observed due to the low solubility of the sample. However, UV−vis−NIR spectroscopy is an alternative way to determine the addition pattern. Pristine $Lu_3N@I_h$-C_{80} and derivative **1** display a maximum absorption at 402 and 404 nm and a weak absorption centered at 674 and 684 nm, respectively, as shown in Figure 4. The absorption spectrum of the $Lu_3N@I_h$-C_{80} methano derivative matches closely the one for pristine $Lu_3N@I_h$-C_{80}, which suggests that the electronic structure of the C_{80} cage is not appreciably altered by addition of the benzal substituent.[9,31] Furthermore, the absorption spectrum of **1** is almost identical to those observed for a series of $Lu_3N@I_h$-C_{80}-PCBM derivatives.[9] These results indicate that this derivative is most likely a fulleroid.[9,31]

On the basis of many reports, the electrochemical behavior of TNT-EMF monoadducts depends mainly on the location of the addends.[4] [5,6]-TNT-EMF adducts exhibit reversible cathodic electrochemical behavior,[23] while [6,6]-adducts exhibit irreversible behavior,[23,30,31] except for the $Sc_3N@I_h$-C_{80} [6,6]-adducts, which display reversible reductive behavior.[33,55] Therefore, electrochemistry can serve as a complementary and diagnostic tool to determine the position of the functional groups on the cage surface.[23] The electrochemical behavior of **1** was recorded in *o*-dichlorobenzene (*o*-DCB) containing 0.05 M *n*-Bu_4NPF_6 as the supporting electrolyte. Figure 5 shows the cyclic voltammogram of **1**. Irreversible cathodic electrochemical behavior with E_{pc} values of −1.49, −1.95, and −2.32 V versus Fc/Fc$^+$ was observed. The reduction potentials of **1** are cathodically shifted by 70, 150, and 60 mV, respectively, compared with those observed for the pristine $Lu_3N@I_h$-C_{80}. Quasi-reversible anodic electrochemical behavior with E_{pa} values of +1.10 and +0.59 V versus Fc/Fc$^+$ was observed. Combining the NMR, UV−vis−NIR absorption, and electrochemical results, compound **1** is most likely the open [6,6]-regioisomer.

Table 1 shows the redox potentials measured for $Lu_3N@I_h$-C_{80} and **1**. The processes for **1** are very similar to those of the $Lu_3N@I_h$-C_{80} Bingel−Hirsch adducts reported by Echegoyen et al.[30] and to those of other cyclopropanated adducts of $Lu_3N@I_h$-C_{80} on the 6,6-bond.[9] Notably, the first oxidation and reduction potentials of **1** are comparable to those observed for $Lu_3N@C_{80}$-PCBM and $Lu_3N@C_{80}$-PCBH, which were shown to be excellent acceptor materials in organic photovoltaic devices.[9] As reported, the increase in the reduction potential is expected to lead to high open-circuit voltages (V_{oc}) and consequently to relatively high efficiencies in OPV devices.[8−10,56,57]

Attempts To Synthesize [Methano-[6,6]-$Sc_3N@I_h$-C_{80}] fullerene. The nucleophilic reaction of $Sc_3N@I_h$-C_{80} dianion with $PhCHBr_2$ was attempted under conditions identical to those used to generate [methano-[6,6]-$Lu_3N@I_h$-C_{80}]fullerene. $[Sc_3N@I_h$-$C_{80}]^{2-}$ was generated under CPE conditions followed by addition of an excess of $PhCHBr_2$ and stirring for the same time used for $[Lu_3N@I_h$-$C_{80}]^{2-}$. The reaction mixture was analyzed using HPLC, and no products were detected, except the recovered starting material, $Sc_3N@I_h$-C_{80}, in 95% yield.

Computational Analysis. DFT calculations were carried out to analyze the different reactivity between $[Sc_3N@I_h$-$C_{80}]^{2-}$ and $[Lu_3N@I_h$-$C_{80}]^{2-}$ and the structure and electronic properties of compound **1**. Theoretical studies for monoreduced $[M_3N@I_h$-$C_{80}]^-$ (M = Sc, Lu) show that most of the spin density of the system is localized in the metal cluster when M = Sc, whereas the spin density is much higher on the carbon cage when M = Lu, in good agreement with the results of EPR experiments.[58−60] The electronic structure of dianions is simpler because all electrons present are paired. The HOMOs of the direduced $M_3N@I_h$-C_{80}

Table 2. Relative, HOMO, and LUMO Energies for Different Orientational Isomers of [6,6]-[$Lu_3N@I_h$-C_{80}-CHPh] and $Lu_3N@I_h$-C_{80}

[6,6]-[$Lu_3N@I_h$-C_{80}-CHPh]	orientation (deg)[a]	E_{rel} (kcal mol^{-1})	E_{HOMO} (eV)	E_{LUMO} (eV)
I1	0	1.1	−5.753	−4.228
I2[b]	45	0.0	−5.733	−4.195
I3[b]	90	1.1	−5.793	−4.246
$Lu_3N@I_h$-C_{80}			−5.909	−4.311

[a] Approximate angle that forms the Lu_3N plane with respect to the plane constituted by the methine carbon of the ligand and the two functionalized carbon atoms of the cage. [b] Isomers I2 and I3 correspond to the orientations denoted as I3 and I4 in ref 31.

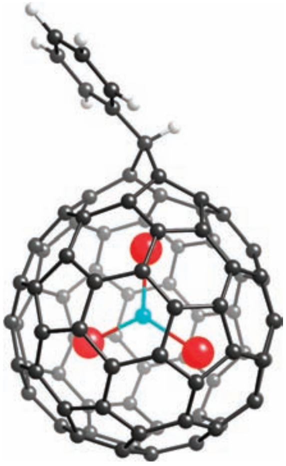

Figure 7. Representation of the structure for the lowest-energy orientational isomer of the [6,6]-[$Lu_3N@I_h$-C_{80}-CHPh] regioisomer. In the optimal structure, the Lu_3N plane forms an angle of approximately 45° with respect to the plane constituted by the methine carbon of the ligand and the two functionalized carbon atoms of the fullerene.

(M = Lu, Sc) show that the contribution of the fullerene cage is more important for M = Lu than for M = Sc for the lowest-energy orientations of the M_3N cluster (Figure 6). It is worth mentioning that computations predict a more hindered rotation of the nitride cluster after one- or two-electron reductions of both Sc- and Lu-endohedral metallofullerenes. Even though some rotation of the nitride might exist, the nature of the HOMOs does not change too much with the orientation of the cluster. Therefore, the less negative charge on the carbon cage accounts for the lower nucleophilic reactivity of the $Sc_3N@I_h$-C_{80} dianion.

For compound **1**, one of the Lu atoms was assumed to be pointing to the functionalized C—C bond according to previous studies on related systems.[31] Three orientational isomers were optimized for which the relative, HOMO, and LUMO energies are given in Table 2. The optimal structure is the open fulleroid (Figure 7), for which the functionalized C—C distance is 2.238 Å in agreement with the spectroscopic and electrochemical conclusion. The [6,6]-closed regioisomer is not found to be a minimum when the M atoms are pointing to the functionalized C—C bond, i.e., the C—C is broken during the structure optimization process. Closed regioisomers were only found for some orientations in which the M atoms of the cluster are not directed to the reacting C—C bond, and they lay at much higher energies (more than 25 kcal mol^{-1}) than the open fulleroid as observed previously for similar systems.[31,61] Given that there are several orientational isomers in a range around 1 kcal·mol^{-1}, we can assume that the Lu_3N cluster can rotate fairly freely around an axis that would cross the open C—C bond and pass along the Lu—N bond. As shown in Table 2 the energies of the HOMO and LUMO change slightly with the position of the trimetallic nitride. The HOMOs of the three isomers of **1** are destabilized with respect to the HOMO of the pristine $Lu_3N@I_h$-C_{80} by about 150 meV, which explains why the first oxidation potential of **1** occurred at a lower positive potential. The shifting in the reduction potentials can also be rationalized easily from the change in the orbital energies of $Lu_3N@I_h$-C_{80} after formation of the adduct. The LUMO energy for **1** is higher than that of the pristine $Lu_3N@I_h$-C_{80}. The LUMO+1 is also shifted to higher energies after functionalization.

CONCLUSION

For the first time we successfully used an electrosynthetic route to generate a $Lu_3N@I_h$-C_{80} derivative using $[Lu_3N@I_h\text{-}C_{80}]^{2-}$ as a reagent. The isolated compound, $Lu_3N@I_h$-C_{80}-(CHC_6H_5), is probably an open 6,6-monoadduct with high regioselectivity, as shown by MALDI-TOF MS, UV—vis—NIR, NMR spectroscopy, cyclic voltammetry, and DFT computations. Surprisingly, under identical conditions $[Sc_3N@I_h\text{-}C_{80}]^{2-}$ failed to react with the electrophile and led only to the unreacted starting compound. The results of DFT computational calculations for both dianions demonstrated that the HOMO is mainly localized on the fullerene cage for $[Lu_3N@I_h\text{-}C_{80}]^{2-}$, whereas for $[Sc_3N@I_h\text{-}C_{80}]^{2-}$, it is mostly localized on the metal cluster. Therefore, $[Lu_3N@I_h\text{-}C_{80}]^{2-}$ is more nucleophilic and consequently more reactive than $[Sc_3N@I_h\text{-}C_{80}]^{2-}$. Calculations of the electronic structures can be regarded as a potential tool to predict the electrochemical reactivity of different TNT-EMF anions with electrophiles. Electrosynthesis provides a novel route for the synthesis of functionalized TNT-EMFs with a diversity of electrophiles designed for various applications.

EXPERIMENTAL SECTION

Materials and Methods. High-purity graphite rods of 6 mm diameter and 15.5 cm length purchased from POCO Graphite, An Entegris Company, Texas, were core drilled to a depth of 13.0 cm (= 6.2 g of shell carbon) and packed with a 2.4 g mixture of graphite powder (1.68 g), lutetium oxide (0.48 g), and copper (0.24 g) with a weight ratio of C/Lu_2O_3/Cu of 7/2/1. The composite rod was annealed at 1000 °C for 12 h and subjected to an arc discharge as an anode in a helium atmosphere (100 Torr) that contained a small amount of NH_3 gas (10 Torr). The raw soot 4.23 g/per rod containing lutetium metallofullerenes was collected and extracted with CS_2 under sonication at room temperature for 3 h. The fullerenes were isolated from polyaromatic hydrocarbons by flash chromatography on silica, eluting with CS_2. The first fraction containing the fullerenes (1.5 mg/rod) was collected, and the solvent was evaporated. The remaining black solid was washed with diethyl ether and dichloromethane in order to remove the remaining empty cage fullerenes. Finally, $Lu_3N@I_h$-C_{80} was purified by selective chemical oxidation with tris(*p*-bromophenyl)aminium hexachloroantimonate (TBAPH). A 0.2 mg amount of $Lu_3N@I_h$-C_{80} was obtained from one rod. Benzal bromide, *o*-DCB, and toluene were used as received. Tetra-*n*-butylammoniumhexafluorophosphate, *n*-Bu_4NPF_6, was recrystallized from absolute ethanol and dried in vacuum before use. The purity of the compound was verified by HPLC using a Varian Prostar 210 equipped with a PBB (4.5 × 250 mm) column and toluene as eluent at a flow rate of 3 mL min^{-1}. MALDI-TOF mass spectrometry was conducted on a Bruker Microflex LRF mass spectrometer. The NMR spectrum was recorded using a 500 MHz Bruker spectrometer. The UV−vis−NIR spectra were taken using a Cary 5000 UV−vis−NIR spectrophotometer. Cyclic voltammetry was carried out in a one-compartment cell connected to a BAS 100B workstation in a solution of *o*-DCB containing 0.05 M *n*-Bu_4NPF_6. A 2 mm diameter glassy carbon disk was used as the working electrode. Ferrocene was added to the solution at the end of each experiment as internal standard.

Synthesis of 1. A 4 mg (3 μmol) amount of sample of $Lu_3N@I_h$-C_{80} was reduced in 15 mL of *o*-DCB and 1 mL of DMF containing 0.05 M *n*-Bu_4NPF_6 as the supporting electrolyte under controlled potential electrolysis (CPE) at −1.60 V versus a silver wire reference electrode under an argon atmosphere. The potentiostat was switched off after the electrogeneration of $[Lu_3N@I_h\text{-}C_{80}]^{2-}$ was completed, a 500-fold excess of benzal bromide ($PhCHBr_2$, 0.2 mL) was then added to the solution in one portion, and the reaction was allowed to proceed for 2 h with stirring. The solvent was evaporated, and ca. 100 mL of methanol was then added to precipitate the product and remove the unreacted benzal bromide. The slurry was separated by filtration, and the residue was put in ca. 25 mL of toluene and sonicated. The soluble fraction was purified by HPLC using a PBB column. A 0.6 mg amount of derivative **1** was obtained, 30% yield based on consumed $Lu_3N@I_h$-C_{80} (2 mg). **1**: ^{1}H NMR (500 MHz, CS_2/CD_3OCD_3, 25 °C, TMS) δ = 7.40 (d, *J* = 8.5 Hz, 2H, Ph−H), 6.86 (t, *J* = 7.5 Hz, 1H, Ph−H), 6.78 (t, *J* = 7.5 Hz, 2H, Ph−H), and 5.37 (s, 1H, C−H) ppm. UV−vis−NIR (toluene): λ = 404 and 684 nm. MALDI-TOF-MS: (positive ionization mode 1,8,9-trihydroxyanthracene as matrix): $[M + H]^+$: 1589.81.

Computational Details. The calculations were carried out using DFT methodology with the ADF 2008 program.[62,63] The exchange-correlation functionals of Becke[64] and Perdew[65] were used. Relativistic corrections were included by means of the ZORA formalism. Triple-zeta and polarization basis sets were employed to describe the valence electrons of C, N, H, and Lu.

■ ASSOCIATED CONTENT

Ⓢ Supporting Information. Complete ref 14; *x,y,z* coordinates for the lowest energy structures studied in this work. This material is available free of charge via the Internet at http://pubs.acs.org.

■ AUTHOR INFORMATION

Corresponding Author

josepmaria.poblet@urv.cat; echegoyen@utep.edu

■ ACKNOWLEDGMENT

Financial support from the National Science Foundation (DMR-0809129 to F.L., J.P., and L.E.) is greatly appreciated. This work was also supported by the Spanish Ministry of Science and Innovation (Project No. CTQ2008-06549-C02-01/BQU and the RyC Program, A.R.-F.) and by the Generalitat de Catalunya (2009SGR462 and XRQTC).

■ REFERENCES

(1) Stevenson, S.; Rice, G.; Glass, T.; Harlch, K.; Cromer, F.; Jordan, M. R.; Craft, J.; Hadju, E.; Bible, R.; Olmstead, M. M.; Maltra, K.; Fisher, A. J.; Balch, A. L.; Dorn, H. C. *Nature* **1999**, *401*, 55–57.

(2) Stevenson, S.; Fowler, P. W.; Heine, T.; Duchamp, J. C.; Rice, G.; Glass, T.; Harich, K.; Hajdu, E.; Bible, R.; Dorn, H. C. *Nature* **2000**, *408*, 427–428.

(3) Dunsch, L.; Yang, S. *Small* **2007**, *3*, 1298–1320.

(4) Chaur, M. N.; Melin, F.; Ortiz, A. L.; Echegoyen, L. *Angew. Chem., Int. Ed.* **2009**, *48*, 7514–7538.

(5) Pinzón, J. R.; Plonska-Brzezinska, M. E.; Cardona, C. M.; Athans, A. J.; Gayathri, S. S.; Guldi, D. M.; Herranz, M. A.; Martín, N.; Torres, T.; Echegoyen, L. *Angew. Chem., Int. Ed.* **2008**, *47*, 4173–4176.

(6) Pinzón, J. R.; Cardona, C. M.; Herranz, M. A.; Plonska-Brzezinska, M. E.; Palkar, A.; Athans, A. J.; Martín, N.; Rodríguez-Fortea, A.; Poblet, J. M.; Bottari, G.; Torres, T.; Gayathri, S. S.; Guldi, D. M.; Echegoyen, L. *Chem.—Eur. J.* **2009**, *15*, 864–877.

(7) Pinzón, J. R.; Gasca, D. C.; Sankaranarayanan, S. G.; Bottari, G.; Torres, T.; Guldi, D. M.; Echegoyen, L. *J. Am. Chem. Soc.* **2009**, *131*, 7727–7734.

(8) Shu, C.; Xu, W.; Slebodnick, C.; Champion, H.; Fu, W.; Reid, J. E.; Azurmendi, H.; Wang, C.; Harich, K.; Dorn, H. C.; Gibson, H. W. *Org. Lett.* **2009**, *11*, 1753–1756.

(9) Ross, R. B.; Cardona, C. M.; Guldi, D. M.; Sankaranarayanan, S. G.; Reese, M. O.; Kopidakis, N.; Peet, J.; Walker, B.; Bazan, G. C.; Van Keuren, E.; Holloway, B. C.; Drees, M. *Nat. Mater.* **2009**, *8*, 208–212.

(10) Ross, R. B.; Cardona, C. M.; Swain, F. B.; Guldi, D. M.; Sankaranarayanan, S. G.; Van Keuren, E.; Holloway, B. C.; Drees, M. *Adv. Funct. Mater.* **2009**, *19*, 2332–2337.

(11) Fatouros, P. P.; Corwin, F. D.; Chen, Z.-J.; Broaddus, W. C.; Tatum, J. L.; Ge, Z.; Gibson, H. W.; Kile, J. L.; Leonard, A. P.; Duchamp, J. C.; Dorn, H. C. *Radiology* **2006**, *240*, 756–764.

(12) Shu, C.; Corwin, F. D.; Zhang, J.; Reid, J. E.; Sun, M.; Xu, W.; Sim, J. H.; Wang, C.-R.; Fatouros, P. P.; Esker, A. R.; Gibson, H. W.; Dorn, H. C. *Bioconjugate Chem.* **2009**, *18*, 1186–1193.

(13) Dorn, H. C.; Reid, J.; Owens, L. S.; Cai, T.; Long, G. L.; Corwin, F. C.; Gibson, H. W.; Shu, C.-Y.; Chen, Z.-J.; Fatouros, P. P.; Zhang, J.-F. *Bioconjugate Chem.* **2010**, *21*, 610–615.

(14) Dorn, H. C.; et al. *Nano Lett.* **2010**, *10*, 2843–2848.

(15) Shultz, M. D.; Duchamp, J. C.; Wilson, J. D.; Shu, C.-Y; Ge, Y.; Zhang, J.; Gibson, H. W.; Fillmore, H. L.; Hirsch, J. I.; Dorn, H. C.; Fatouros, P. P. *J. Am. Chem. Soc.* **2010**, *132*, 4980–4981.

(16) Zhang, E. Y.; Shu, C. Y.; Feng, L.; Wang, C. R. *J. Phys. Chem. B* **2007**, *111*, 14223–14226.

(17) Braun, K.; Dunsch, L.; Pipkorn, R.; Bock, M.; Baeuerle, T.; Yang, S. F.; Waldeck, W.; Wiessler, M. *Int. J. Med. Sci.* **2010**, *7*, 136–146.

(18) Iezzi, E. B.; Duchamp, J. C.; Harich, K.; Glass, T. E.; Lee, H. M.; Olmstead, M. M.; Balch, A. L.; Dorn, H. C. *J. Am. Chem. Soc.* **2002**, *124*, 524–525.

(19) Lee, H. M.; Olmstead, M. M.; Iezzi, E.; Duchamp, J. C.; Dorn, H. C.; Balch, A. L. *J. Am. Chem. Soc.* **2002**, *124*, 3494–3495.

(20) Cardona, C. M.; Kitaygorodskiy, A.; Ortiz, A.; Herranz, M. A.; Echegoyen, L. *J. Org. Chem.* **2005**, *70*, 5092–5097.

(21) Cai, T.; Ge, Z.; Iezzi, E. B.; Glass, T. E.; Harich, K.; Gibson, H. W.; Dorn, H. C. *Chem. Commun.* **2005**, 3594–3596.

(22) Cardona, C. M.; Kitaygorodskiy, A.; Echegoyen, L. *J. Am. Chem. Soc.* **2005**, *127*, 10448–10453.

(23) Cardona, C. M.; Elliott, B.; Echegoyen, L. *J. Am. Chem. Soc.* **2006**, *128*, 6480–6485.

(24) Campanera, J. M.; Bo, C.; Poblet, J. M. *J. Org. Chem.* **2006**, *71*, 46–54.

(25) Chen, N.; Zhang, E. Y.; Tan, K.; Wang, C. R.; Lu, X. *Org. Lett.* **2007**, *9*, 2011–2013.

(26) Chen, N.; Fan, L. Z.; Tan, K.; Wu, Y. Q.; Shu, C. Y.; Lu, X.; Wang, C. R. *J. Phys. Chem. C* **2007**, *111*, 11823–11828.

(27) Cai, T.; Slebodnick, C.; Xu, L.; Harich, K.; Glass, T. E.; Chancellor, C.; Fettinger, J. C.; Olmstead, M. M.; Balch, A. L.; Gibson, H. W.; Dorn, H. C. *J. Am. Chem. Soc.* **2006**, *128*, 6486–6492.

(28) Cai, T.; Xu, L.; Anderson, M. R.; Ge, Z.; Zuo, T.; Gibson, H. W.; Dorn, H. C. *J. Am. Chem. Soc.* **2006**, *128*, 8581–8589.

(29) Shu, C. Y.; Cai, T.; Xu, L. S.; Zuo, T. M.; Reid, J.; Harich, K.; Dorn, H. C.; Gibson, H. W. *J. Am. Chem. Soc.* **2007**, *129*, 15710–15717.

(30) Pinzón, J. R.; Zuo, T. M.; Echegoyen, L. *Chem.—Eur. J.* **2010**, *16*, 4864–4869.

(31) Lukoyanova, O.; Cardona, C. M.; Rivera, J.; Lugo-Morales, L. Z.; Chancellor, C. J.; Olmstead, M. M.; Rodriguez-Fortea, A.; Poblet, J. M.; Balch, A. L.; Echegoyen, L. *J. Am. Chem. Soc.* **2007**, *129*, 10423–10430.

(32) Chaur, M. N.; Melin, F.; Athans, A. J.; Elliott, B.; Walker, K.; Holloway, B. C.; Echegoyen, L. *Chem. Commun.* **2008**, 2665–2667.

(33) Li, F.-F.; Pinzón, J. R.; Mercado, B. Q.; Balch, A. L.; Echegoyen, L. *J. Am. Chem. Soc.*, DOI:10.1021/ja1097176.

(34) Iiduka, Y.; Ikenaga, O.; Sakuraba, A.; Wakahara, T.; Tsuchiya, T.; Maeda, Y.; Nakahodo, T.; Akasaka, T.; Kako, M.; Mizorogi, N.; Nagase, S. *J. Am. Chem. Soc.* **2005**, *127*, 9956–9957.

(35) Wakahara, T.; Iiduka, Y.; Ikenaga, O.; Nakahodo, T.; Sakuraba, A.; Tsuchiya, T.; Maeda, Y.; Kako, M.; Akasaka, T.; Yoza, K.; Horn, E.; Mizorogi, N.; Nagase, S. *J. Am. Chem. Soc.* **2006**, *128*, 9919–9925.

(36) Shustova, N. B.; Popov, A. A.; Mackey, M. A.; Coumbe, C. E.; Phillips, J. P.; Stevenson, S.; Strauss, S. H.; Boltalina, O. V. *J. Am. Chem. Soc.* **2007**, *129*, 11676–11677.

(37) Shu, C. Y.; Slebodnick, C.; Xu, L. S.; Champion, H.; Fuhrer, T.; Cai, T.; Reid, J. E.; Fu, W.; Harich, K.; Dorn, H. C.; Gibson, H. W. *J. Am. Chem. Soc.* **2008**, *130*, 17755–17760.

(38) Echegoyen, L.; Echegoyen, L. E. *Acc. Chem. Res.* **1998**, *31*, 593–601.

(39) Reed, C. A.; Bolskar, R. D. *Chem. Rev.* **2000**, *100*, 1075–1120.

(40) Caron, C.; Subramanian, R.; D'Souza, F.; Kim, J.; Kunter, W.; Jones, M. T.; Kadish, K. M. *J. Am. Chem. Soc.* **1993**, *115*, 8505–8506.

(41) Boulas, P. L.; Zuo, Y.; Echegoyen, L. *Chem. Commun.* **1996**, 1547–1548.

(42) Kadish, K. M.; Gao, X.; Van Caemelbecke, E.; Hirasaka, T.; Suenobu, T.; Fukuzumi, S. *J. Phys. Chem. A* **1998**, *102*, 3898–3906.

(43) Kadish, K. M.; Gao, X.; Van Caemelbecke, E.; Suenobu, T.; Fukuzumi, S. *J. Am. Chem. Soc.* **2000**, *122*, 563–570.

(44) Kadish, K. M.; Gao, X.; Van Caemelbecke, E.; Suenobu, T.; Fukuzumi, S. *J. Phys. Chem. A* **2000**, *104*, 3878–3883.

(45) Kadish, K. M.; Gao, X.; Gorelik, O.; Caemelbecke, E. V.; Suenobu, T.; Fukuzumi, S. *J. Phys. Chem. A* **2000**, *104*, 2902–2907.

(46) Zheng, M.; Li, F. F.; Shi, Z. J.; Gao, X.; Kadish, K. M. *J. Org. Chem.* **2007**, *72*, 2538–2542.

(47) Yang, W.-W.; Li, Z.-J.; Gao, X. *J. Org. Chem.* **2010**, *75*, 4086–4094.

(48) Zheng, M.; Li, F.-F.; Ni, L.; Yang, W.-W.; Gao, X. *J. Org. Chem.* **2008**, *73*, 3159–3168.

(49) Li, F.-F.; Yang, W.-W.; He, G.-B.; Gao, X. *J. Org. Chem.* **2009**, *74*, 8071–8077.

(50) Li, F.-F.; Gao, X.; Zheng, M. *J. Org. Chem.* **2009**, *74*, 82–87.

(51) Campanera, J. M.; Bo, C.; Olmstead, M. M.; Balch, A. L.; Poblet, J. M. *J. Phys. Chem. A* **2002**, *106*, 12356–12364.

(52) Krause, M.; Kuzmany, H.; Georgi, P.; Dunsch, L.; Vietze, K.; Seifert, G. *J. Chem. Phys.* **2001**, *115*, 6596–6605.

(53) Alvarez, L.; Pichler, T.; Georgi, P.; Schwieger, T.; Peisert, H.; Dunsch, L.; Hu, Z.; Knupfer, M.; Fink, J.; Bressler, P.; Mast, M.; Golden, M. S. *Phys. Rev. B* **2002**, *66*, 035107/1–035107/7.

(54) Chaur, M. N.; Valencia, R.; Rodriguez-Fortea, A.; Poblet, J. M.; Echegoyen, L. *Angew. Chem., Int. Ed.* **2009**, *48*, 1425–1428.

(55) Chen, N.; Pinzón, J. R.; Echegoyen, L. Revised for publication.

(56) Kooistra, F. B.; Knol, J.; Kastenberg, F.; Popescu, L. M.; Verhees, W. J. H.; Kroon, J. M.; Hummelen, J. C. *Org. Lett.* **2007**, *9*, 551–554.

(57) Lenes, M.; Wetzelaer, Gert-Jan A. H.; Kooistra, F. B.; Veenstra, S. C.; Hummelen, J. C.; Blom, P. W. M. *Adv. Mater.* **2008**, *20*, 2116–2119.

(58) Chaur, M. N.; Aparicio-Anglés, X.; Mercado, B. Q.; Elliott, B.; Rodríguez-Fortea, A.; Clotet, A.; Olmstead, M. M.; Balch, A. L.; Poblet, J. M.; Echegoyen, L. *J. Phys. Chem. C* **2010**, *114*, 13003–13009.

(59) Popov, A. A.; Dunsch, L. *J. Am. Chem. Soc.* **2008**, *130*, 17726–17742.

(60) Valencia, R.; Rodríguez-Fortea, A.; Clotet, A.; de Graaf, C.; Chaur, M. N.; Echegoyen, L.; Poblet, J. M. *Chem.—Eur. J.* **2009**, *15*, 10997–11009.

(61) Alegret, N.; Chaur, M. N.; Santos, E.; Rodríguez-Fortea, A.; Echegoyen, L.; Poblet, J. M. *J. Org. Chem.* **2010**, *75*, 8299–8302.

(62) *ADF 2008.01*; Department of Theoretical Chemistry, Vrije Universiteit: Amsterdam, 2008.

(63) Velde, G. T.; Bickelhaupt, F. M.; Baerends, E. J.; Guerra, C. F.; Van Gisbergen, S. J. A.; Snijders, G.; Ziegler, T. *J. Comput. Chem.* **2001**, *22*, 931–967.

(64) Becke, A. D. *Phys. Rev. A* **1988**, *38*, 3098–3100.

(65) Perdew, J. P. *Phys. Rev. B* **1986**, *33*, 8822–8824.